

EFFECT OF TRIANGULAR VORTEX GENERATOR TO CONTROL FLOW SEPARATION

Md. Hasan Ali^{1*}, B. M. Asaduzzaman² and Mohammad Mashud³

¹Department of Energy Technology

^{2,3}Department of Mechanical Engineering
Khulna University of Engineering & Technology
Khulna-9203, Bangladesh

E-mail: mhakueta@yahoo.com*, mdmashud@yahoo.com

Abstract- An experimental wind tunnel study of the flow past a row of counter-rotating vortex generators mounted on top of a bump has been performed. All three velocity components are measured in spanwise planes downstream of the vortex generators using Stereoscopic Particle Image Velocimetry, SPIV. The flow behaves as expected, in the sense that the vortices transport high momentum fluid into the boundary layer, making it thinner and more resistant to the adverse pressure gradients with respect to separation. The idea behind the experiments is that the results will be offered for validation of modeling of the effect of vortex generators with various numerical codes.

Keywords: Flow separation, Vortex generator and Triangular VG

1. INTRODUCTION

For some industrial flows it is beneficial to transfer high momentum fluid from the outer flow into the boundary layer in order to increase e.g. the fluid temperature near a wall in a heat exchanger or to increase momentum to a boundary layer exposed to an adverse pressure gradient in order to delay separation. This mixing can e.g. be achieved by increasing the turbulence using so-called turbulators, or by creating a vortex structure in the streamwise direction that by convection mixes the flow. In reality both effects are probably occurring. Taylor introduced so-called vortex generators in 1947 [1], which is basically a small rectangular or triangular plate glued to the surface with an angle of incidence to the main flow, see Figure 1.

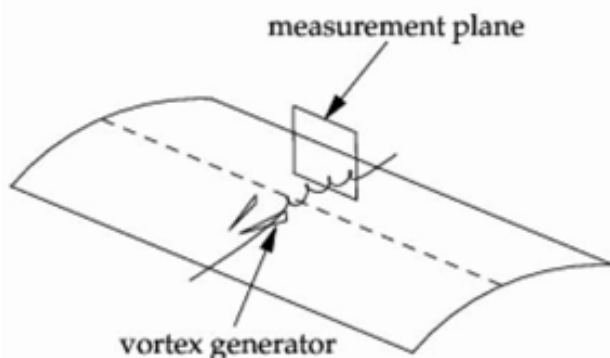


Figure 1: Vortex generator pair and the positioning of measurement planes

These plates act as small wings and the tip vortices are convected downstream and mix high momentum or high temperature flow into the boundary layer. One would expect that the height of the vortex generator should be approximately the boundary layer height, δ , but Lin [2] shows that for a turbulent flow they can have a large effect even at a height of approximately 0.2δ , since the streamwise velocity gradient is very high in a turbulent boundary layer. This type of vortex generators are denoted submerged, low profile or micro VGs. Vortex generators can be placed to create co- or counter-rotating vortices (see Figure 2) and it is shown in Godard and Stanislas [3] that they work most efficiently when creating counter-rotating vortices.

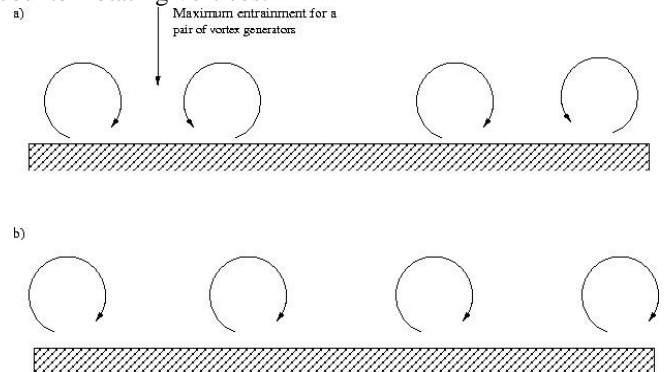


Figure 2: Vortices seen from behind a) counter-rotating and b) co-rotating vortex generators

In [3] various experiments are performed to further estimate an optimum geometry of the vortex generators. This optimum geometry will of course depend on the application and is therefore most likely not universal, but has nevertheless also been used in our experiment. The use of vortex generators on wind turbine blades can in some cases have quite a dramatic influence on the produced power (see [4]) and they are therefore often used on commercial wind turbine blades. The main purpose in the present work is to create a detailed database of the flow behind vortex generators in a controlled experiment in order to be used for later code validation.

2. METHODOLOGY

The measurements were carried out in a closed-circuit wind tunnel with an 8:1 contraction ratio and a test section of cross sectional area 300 x 600 mm with length 2 m. The experiments were conducted at a free stream velocity $U_\infty = 1$ m/s, corresponding to $R = 20\,000$ based on the bump chord length. The turbulent inflow is assured by a turbulence generating inlet grid with mesh length $M=39$ mm situated at the beginning of the test section. In [5] the turbulence intensity at the inlet is estimated to 12% and the boundary layer thickness at the VG position is measured to be 25 mm. The suction side of the wind turbine wing is represented by a bump mounted vertically on one of the test section walls with the leading edge positioned 600 mm downstream of the inlet grid. The bump is a circular sector, extended in the spanwise direction creating a cylindrical sector with radius 390 mm. The bump height is 30 mm and the chord length and bump width are 300 mm and 600 mm respectively. The vortex generators were positioned with their trailing edges at 42% bump chord. The vortex generators are triangular and their height is 1δ , where δ represents the boundary layer thickness at the position of the vortex generators. The length of the vortex generators are twice their height and the device angle of incidence is 18° . The measurements were conducted in spanwise planes (see Figure 1) at various positions downstream of the vortex generators. A sketch of the wind tunnel test section and the positioning of measurement planes is shown in Figure 3, where also the coordinate system is defined. The equipment was mounted on a rigid traverse, traversing in the heightwise and streamwise directions. This configuration enables one to calibrate only once and perform measurements accurately at the different positions using the same calibrated configuration.

A sketch of the experimental setup is found in Figure 4. The laser was placed at the top of the test section, illuminating the vertically mounted bump from the side. The two cameras were placed on the same side of the light sheet, resulting in one camera placed in the forward scattering direction and one in the backward scattering one.

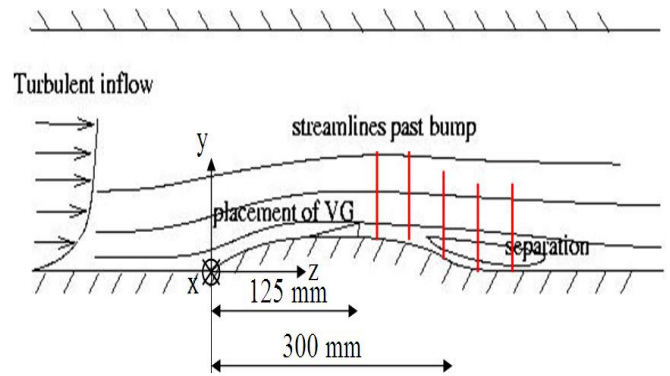


Figure 3: Sketch of bump and definition of coordinate system

The angle of each respective camera to the laser sheet was 45° . The f-numbers were set to between 8 and 16 for the camera in the forward scattering direction and 4 or 5.6 for the camera in the backward scattering direction, depending on the light budget at each individual plane. The stereoscopic PIV equipment included a double cavity Solo 120 XT Nd-YAG laser (wavelength 532 nm) capable of delivering light pulses of 120 mJ. The light sheet thickness at the measurement position of 2 mm was created using a combination of a spherical convex and a cylindrical concave lens. The equipment also included two Dantec Dynamics HiSense MkII cameras (1344 x 1024 pixels) equipped with 60 mm lenses and filters designed to only pass light with wavelengths close to that of the laser light. Both cameras were mounted on Scheimpflug angle adjustable mountings. In order to obtain a smaller measurement area, the cameras were equipped with teleconverters. The seeding, consisting of 2-3 μm glycerol droplets, was added to the flow downstream of the test section. The images were processed using Dantec Flowmanager software version 4.7. Adaptive correlation was applied using refinement with an initial and final interrogation area size of 64x64 and 32x32 pixels respectively. Local median validation was used in the immediate vicinity of each vector to remove spurious vectors between each refinement step. The overlap between interrogation areas was 50%. For each measurement position, a sample size of 500 was chosen. The recording of image maps was done with an acquisition rate of 1.0 Hz. In order to provide the cameras with the information for reconstruction of the velocity vectors to three component velocities, a calibration was performed. A calibration target was positioned within the light sheet and traversed through the streamwise direction in steps of 0.5 mm through five different positions which were recorded by the two cameras. The mapping function, providing the transformation from the coordinate system of the respective camera to the coordinate system of the calibration target, was obtained from these recordings using a linear transformation.

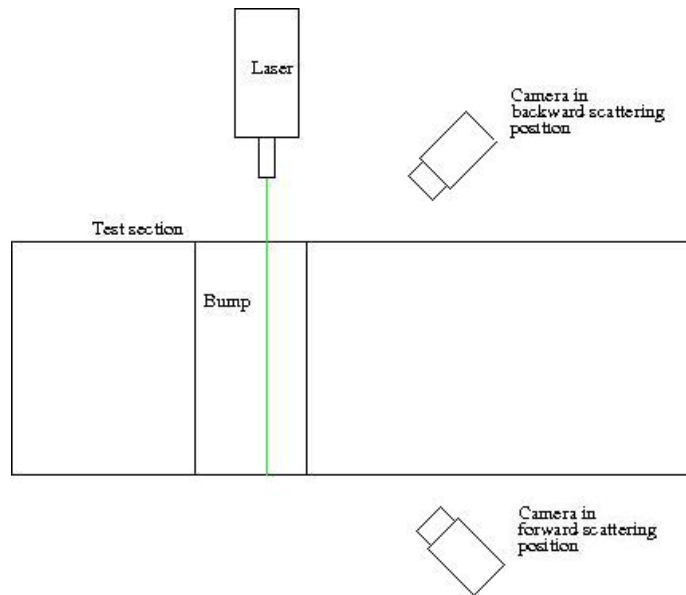
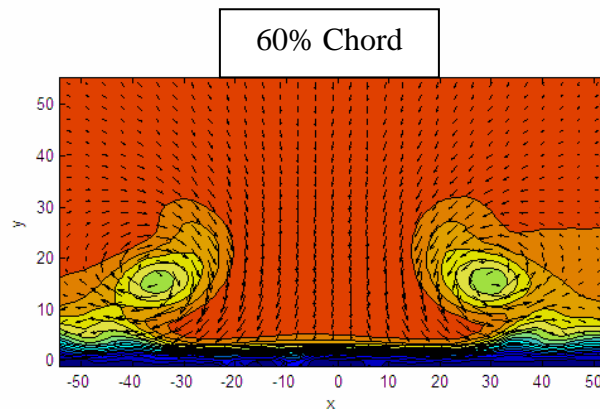


Figure 4: Sketch of experimental set up

3. RESULTS AND DISCUSSION

The mean velocity of the measurements for four positions downstream of the vortex generators are shown in Figure 5 as a combination of velocity vectors and color plots. The color indicates the out of plane velocity (main flow) and the vectors indicate the secondary flow induced by the vortex generators. Only every fourth vector is shown in these plots, whose downstream positions are shown in terms of percentage of chord length downstream of the leading edge of the bump. One can clearly see that the vortex generators have a strong visible effect on the boundary layer. It is very clear looking at the out-of-plane component, how

high momentum fluid is being transferred into the near wall region in the downwash region and that the boundary layer thus becomes very thin in between these counter-rotating vortices induced by a vortex generator pair. It is also seen how this effect is reduced when moving downstream. Figure 6 shows the measured streamwise velocity component at different streamwise positions in the configurations with and without vortex generators in the symmetry plane ($x=0$). It is again seen that the transfer of high momentum into the boundary layer from the vortex generators decreases the separation behind the bump.



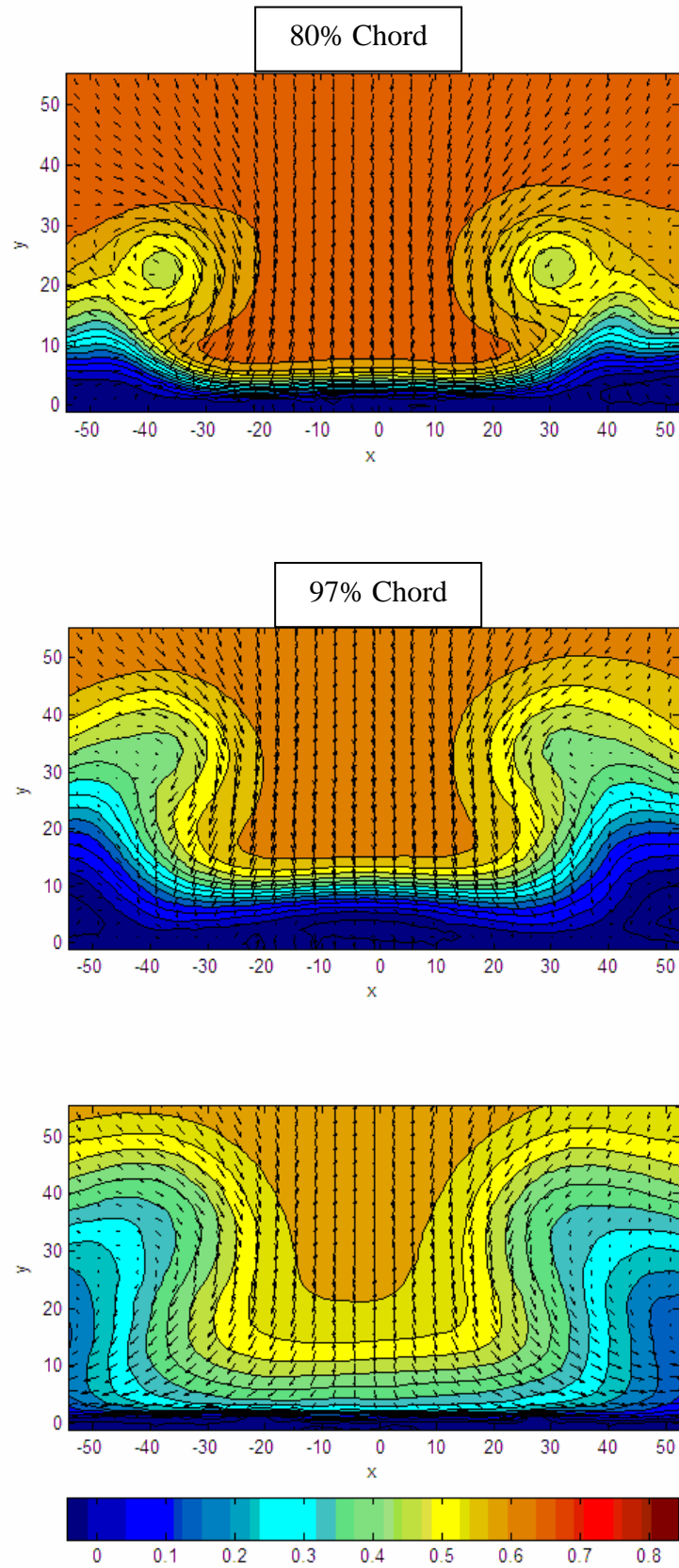


Figure 5: Velocity vector plots. Arrows represent the in-plane velocities and color represents the out-of-plane velocities. The downstream position is given in percentage of chord from the bump leading edge. The vortex generators end at 42%. Every fourth vector is shown in the present plots and the downstream positions are shown in terms of percentage of chord length downstream of the leading edge of the bump.

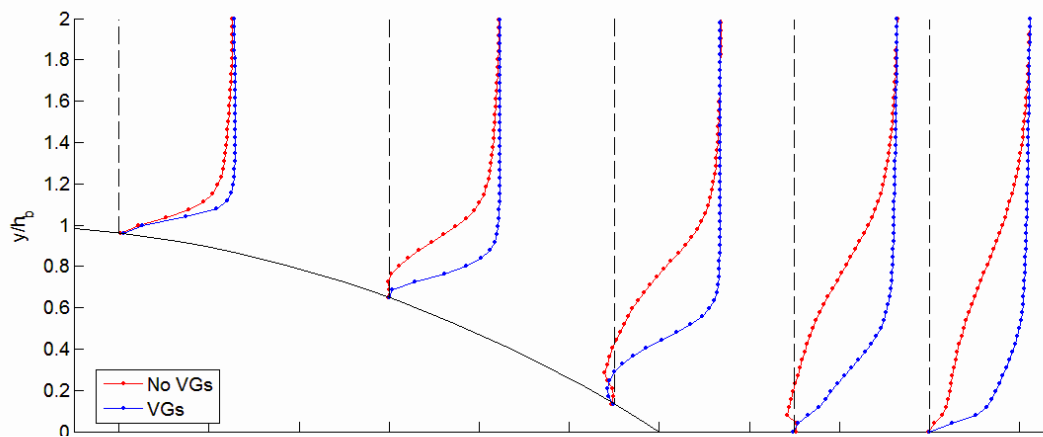


Figure 6: Streamwise velocities at five positions downstream of the vortex generator positions extracted at $x=0$. The red points show the case without vortex generators and the blue ones show the velocity profile in the downwash region of the vortex generators, where the separation reducing effect of the vortex generators is expected

4. CONCLUSION

It has been shown that it is possible to measure and resolve the flow created by a row of vortex generator pairs inducing counter-rotating vortices and their effect on the boundary layer using SPIV. It is apparent from the results that the vortex generators have the expected effect on the flow in the sense that they create large scale mixing near the wall. The measurements clearly show a structured vortex behind each vortex generator, whose development can be traced throughout the downstream planes. In the future these measurements will be used to validate various numerical methods for calculating the flow behind vortex generators.

5. REFERENCES

- [1]. Taylor HD. The elimination of diffuser separation by vortex generators. Aircraft Corporation Report, R-4012-3, June 1947
- [2]. Lin JC. Review of research on low-profile vortex generators to control boundary-layer separation. *Progress in Aerospace Sciences* 38(2002) 389-420
- [3]. Godard G and Stanislas M. Control of a decelerating boundary layer. Part 1: Optimization of passive vortex generators. *Aerospace Science and Technology* 10(2006) 181-191
- [4]. Øye S. The effect of Vortex Generators on the performance of the ELKRAFT 1000 kW Turbine, 9th IEA Symp. On Aerodynamics of Wind Turbines, 1995.
- [5]. Schmidt J.J. Experimental and numerical investigation of separated flows. PhD thesis, Technical University of Denmark, Fluid Mechanics Section, Lyngby, Denmark 1997.